Available online at www.sciencedirect.com
SCIENCE DIRECT®
GEOTHERMICS
ELSEVIER
Geothermics xxx (2006) xxx–xxx
www.elsevier.com/locate/geothermics

A new and fast method to determine mixing and conductive cooling of thermal waters in carbonate-evaporite environments

Stéphanie Levet, Gilles Berger *, Marguerite Munoz, Jean-Paul Toutain

Laboratoire des Mécanismes de Transfert en Géologie, Observatoire Midi-Pyrénées, 14 Av. E. Belin, 31400 Toulouse, France

Received 3 May 2005; accepted 7 March 2006

Abstract

A method is proposed, for low-temperature geothermal systems, for calculating the aquifer temperature and relative proportions of mixed thermal and shallow groundwaters from carbonate-evaporite environments. The fluid is assumed to be in chemical equilibrium with anhydrite and chalcedony in the aquifer, and mixed with diluted waters during its ascent. An attempt has been made to establish a relationship between reservoir temperature, the aqueous sulfate and silica contents of the mixed fluid, the proportion of the thermal end-member and the temperature of the adiabatic mixture. The method calculates mineral solubilities in the field context, calibrated on representative thermal springs. The method also considers the effects of conductive cooling.

Keywords: Low-to medium enthalpy resources; Thermal springs; Mixing process; Conductive cooling; Carbonates; Evaporites

1. Introduction

Numerous geothermometers based on water-rock chemical equilibrium are available in the literature (White et al., 1956; Fournier and Rowe, 1966; Fournier and Truesdell, 1973; Paces, 1975; Fournier, 1977, 1979; Ellis, 1979; Fournier and Potter, 1979, 1982; Fouillac and Michard, 1981; Arnórsson et al., 1983; Giggenbach, 1988; Kharaka and Mariner, 1989; Verma and Santoyo, 1997; Verma, 2001; Can, 2002). These geothermometers provide realistic temperature estimates

* Corresponding author. Tel.: +33 5 6133 2582; fax: +33 5 6133 2560.
E-mail address: berger@lmtg.obs-mip.fr (G. Berger).

0375-6505/$30.00 © 2006 Published by Elsevier Ltd on behalf of CNR.
doi:10.1016/j.geothermics.2006.03.002

in deep crustal environments, where the presence of silica polymorphs and aluminosilicates, and fast equilibration kinetics, allow us to use aqueous silica and cation activity ratios.

Theoretically, any constituent controlled by a temperature-dependent reaction can be used as a geothermometer, under the basic assumption that chemical equilibrium is attained in the geothermal reservoir at depth. However, additional secondary processes such as conductive cooling, boiling, cation exchange on clays, CO_2 degassing, mixing with shallower and cooler groundwaters and gain or loss of steam, may modify the chemistry of the ascending fluids and lead to erroneous interpretations (Fournier and Truesdell, 1974; Arnórsson, 1983). In order to account for some of these processes, Reed and Spycher (1984) have proposed a method that uses the chemical composition of the water to find the temperature at which a group of plausible alteration minerals are assumed to simultaneously control the solution chemistry. This method enables an estimate of the amount of lost gas or diluting waters responsible for the departure of thermal solutions from equilibrium with minerals in the reservoir rocks. It yields good predictions of equilibrium temperatures for hot springs ($T > 150\,^{\circ}C$) and formation waters circulating in granitic, volcanic and mixed lithologies. More recently, Pang and Reed (1998) have improved the approach of Reed and Spycher (1984) by correcting the effects of errors in aluminium analyses or lack of them, which may greatly modify the concentrations of dissolved constituents by taking into account clay minerals/water interactions.

In a sedimentary environment, the mineralogy of the host rocks and the low prevailing temperatures (<150 °C) lead to slow kinetics, with the result that cation geothermometers based on equilibrium with K-feldspars and Ca-bearing silicates cannot be applied. Therefore, under these conditions, silica geothermometers are generally used, although there may at times be some ambiguity in determining which silica mineral (quartz or chalcedony: Arnórsson, 1975; clays: Kharaka and Mariner, 1989) controls the dissolved silica concentration in the reservoir. Moreover, precipitation of silica colloids or Fe-bearing silicates may occur near the surface because of conductive cooling (Degueldre et al., 1996; Palandri and Reed, 2001), as well as clay/water interactions at the surface (Reed and Spycher, 1984; Pang and Reed, 1998).

In the case of low-to-medium temperature (40–180 °C) carbonate-evaporite systems, where calcite, dolomite, anhydrite and fluorite are ubiquitous minerals, Marini et al. (1986) proposed two temperature functions based on Ca^{2+}/Mg^{2+} and SO_4^{2-}/F^- ratios. This model was improved by Chiodini et al. (1991, 1995) by taking into account the effect of ion associations in the saline fluids. More recently, and following the approach of Reed and Spycher (1984) and Pang and Reed (1998), Pastorelli et al. (1999) have proposed combining the solubility of anhydrite and chalcedony in order to estimate the reservoir temperature of waters circulating in Triassic evaporites. None of these methods, however, considers subsurface processes such as conductive cooling and mixing, which can modify the chemical speciation of the ascending fluids considerably, resulting in erroneous equilibrium temperatures. The solubility values also depend upon factors such as pressure, pH, presence of crystal defects, grain size and salinity, which are always fundamental parameters for understanding the chemical characteristics and evolution of hydrothermal systems.

The above is just a brief review of the difficulties encountered when geothermometric equations are applied to complex natural hydrothermal systems. Here, we will address a specific aspect of water/rock interactions in a carbonate-evaporite environment, that is, the dilution of thermal waters by shallow, cooler and less saline groundwaters. This phenomenon is of primary importance in aqueous geothermometry and hydrodynamic modelling. As pointed out by Reed and Spycher (1984) and Palandri and Reed (2001), during the ascent of thermal waters, a process facilitated by the high permeability of the sedimentary rocks and faults/fractures, the chemical composition of the waters is frequently changed by mixing with cold and weakly mineralized

waters (TDS < 0.3 g/l). In their method, Reed and Spycher (1984) first define the dilution proportions as the measured/theoretical concentration ratio, with the theoretical concentrations resulting from the reconstruction of the deep fluid composition, assuming that a group of realistic minerals converges towards equilibration within the aquifer (see also Hull et al., 1987). The mixing problem can also be solved, as proposed by Antroddicchia et al. (1985) and Cioni et al. (1992), by defining binary mass equations based on ion concentrations and isotopic compositions, provided that one of the end-members is known and that no secondary precipitation/dissolution processes affect the chemistry of the fluid during its ascent. Marini et al. (1986) followed a different approach; they adjust ion concentrations until their temperature functions give the same temperature at depth.

These methods require extensive mineralogical and thermodynamic studies and are consequently tedious and time-consuming. One alternative is to improve the methods based on (i) a restricted number of mineral phases, and (ii) the reconstruction of the reservoir fluid chemistry from the chemical composition measured at the spring.

We propose a simplified numerical solution adapted to low-temperature (40–100 °C) carbonate-evaporite environments that can be easily used in real-time with an Excel-type spreadsheet. To validate this method, we have calculated the dilution factors and evaluated the extent of conductive cooling in various carbonate-evaporite aquifers described in the literature, and compared the results.

2. Proposed method: description and basic assumptions

In carbonate-evaporite rocks, the thermal fluid is clearly assumed to have equilibrated with respect to Ca and Mg-carbonates, but we also assume it has done so with anhydrite and chalcedony. For the common range of pH values (6–8) in groundwaters, Ca-bearing carbonates are much less soluble than anhydrite, so the waters display a dominant $CaSO_4$ character with an approximate equivalence between Ca^{2+} and SO_4^{2-} concentrations. Anhydrite and chalcedony exhibit a poor or no solubility dependence on pH, a parameter that changes by degassing of acid gases such as H_2S and CO_2, so that the concentrations of Si, Ca and SO_4 should be conservative, provided the fluid does not undergo dilution by shallow waters. On the other hand, these minerals display opposite behaviours with temperature: chalcedony solubility increases with temperature, while anhydrite displays retrograde solubility. These contradictory features can be used as an efficient tool for estimating the mineral equilibration temperature. As shown by Pastorelli et al. (1999), the temperature of a reservoir can be estimated from the measured chemical composition of the fluid, provided that the sampled fluid was not diluted near the surface.

For a given fluid composition, the method consists of calculating the saturation state of the fluid with respect to anhydrite and chalcedony as a function of temperature. The saturation index (SI) increases with temperature for anhydrite, whereas it decreases for chalcedony. The saturation index (SI) is defined here as $SI = \log(\Omega)$, where Ω is the ionic activity product divided by the solubility constant K. The equilibration temperature in the deep reservoir is assumed to correspond to the temperature for which the two saturation indexes appear simultaneously close to zero (Fig. 1). The temperature calculated as indicated above is based on thermodynamic considerations and uses the activity of the aqueous species and solubility products for the mineral phases. These data can be picked up from standard databases. However, the pure and ideal sulfate and silica minerals described in thermodynamic databases are not exactly representative of the phases controlling fluid composition in nature. In the case of silica, numerous polymorphs or various degrees of crystallinity (amorphous silica, α and β cristobalite, chalcedony) may control aqueous silica concentration, which makes it very difficult to interpret silica concentrations measured in

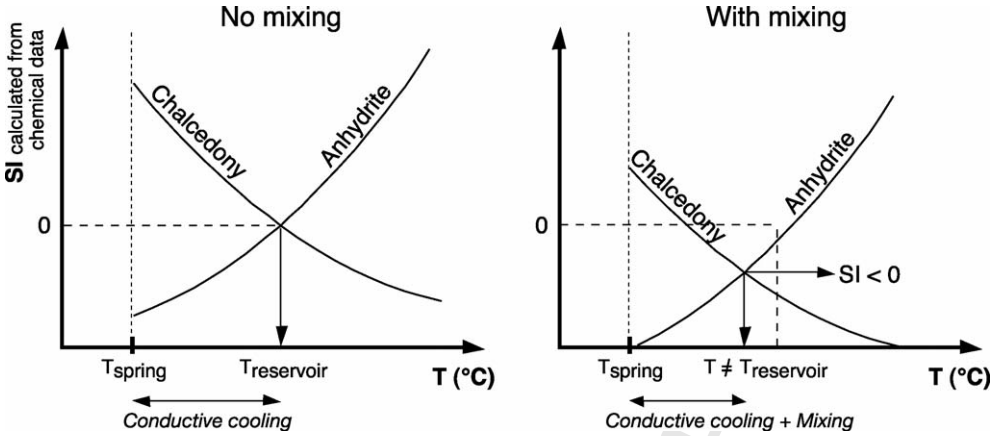

Fig. 1. Temperature vs. saturation index (SI) with respect to anhydrite and chalcedony diagrams, showing the effects of mixing on mineral solubilities and hydrothermal fluids during ascent and cooling.

sedimentary fluids. For example, the silica saturation indexes of the carbonated Dogger aquifer (55–85 °C; Azaroual et al., 1997) cannot be explained by quartz or chalcedony solubilities, and the authors conclude that aqueous silica was probably controlled by an intermediate silica phase. This is less of a problem for $CaSO_4$, since anhydrite is likely to be the unique controlling phase.

In any case, the saturation index estimate should take into account the physical and chemical conditions prevailing in the system. For anhydrite, Ca activity is extremely sensitive to ionic strength and also to the formation of ion pairs such as $CaCO_3^0$ and $CaHCO_3^-$, with the result that the activity depends on the entire fluid composition. The most accurate thermodynamic approach to calculating fluid saturation with respect to anhydrite is the Pitzer (1973) formalism, which integrates the specific interactions between all of the major components of the solution. Unfortunately, the current "Pitzer databases" are poorly documented and the conventional approach based on the Debye-Hückel formalism (Debye and Hückel, 1923) is still the only method available for HCO_3–SO_4 solutions at elevated temperature.

In the case of silica, which is mainly present as neutral species, the difficulty is more the aqueous speciation dependence on pH than the activity coefficient calculation. Above a pH of 5, the proportion of the anionic form $H_3SiO_4^-$ increases significantly with pH, and an accurate calculation of saturation index requires an estimate of the in situ pH, which is reputedly no simple task. However, the pH effect on chalcedony solubility is small below pH 8. Pressure effects should also not be neglected. Millero (1982) and Monnin (1990) predicted, from partial molar volume and compressibility data, a solubility increase of amorphous silica and anhydrite of several tens of percent for pressures between 1 and 100 bars.

Another source of inaccuracy is the mixing of the thermal fluid with shallow groundwaters. Such mixing is ordinarily a dilution of the dissolved cations and anions, since thermal fluids in carbonate-evaporite systems are generally much more concentrated solutions than shallow waters. Mixing will lead to erroneous temperature estimates, as deduced from the solubilities of anhydrite and chalcedony, but with the opposite effect, i.e., an overestimated temperature from anhydrite and an underestimated temperature from chalcedony. This phenomenon is illustrated in Fig. 1, which shows that the SI curves will not cross at SI = 0 for both chalcedony and anhydrite when mixing occurs.

The method developed below allows calculation of the dilution factor for mixed fluids, and consequently yields a better estimate of the reservoir temperature under these conditions. A knowledge of the composition of the deep fluid is not required; it is based on two empirical parameters that should be adjusted for each hydrothermal system so it cannot be termed a real geothermometer. The method consists of defining a simple array of equations that can be solved analytically by means of measured fluid chemical data and considering the dilution factor as an unknown parameter. The equation array is based on the temperature-solubility relationship of anhydrite and chalcedony.

2.1. Step I: expression for the ideal case

For chalcedony, the silica concentration versus temperature relation is easily expressed as a polynomial function by fitting the solubility data in pure water. For anhydrite, we consider as the ideal case a dilute solution with a 1:1 Ca/SO_4 molal ratio. The solubility-temperature dependence can be restricted to the SO_4^{2-} versus temperature relation described by a two-order polynomial function in the 20–100 °C range. The EQ3/6 software package with the SUPCRT92 thermodynamic database (Johnson et al., 1992; Wolery and Daveler, 1992) was used to calculate the aqueous sulfate and silica concentrations at various temperatures. The polynomial forms for the theoretical molal concentrations $[SO_4{}^{2-}]_{th}$ and $[SiO_2aq]_{th}$ were calculated with an Excel spread-sheet and are given by:

$$T\,(^\circ\mathrm{C}) = 0.1176[SO_4^{2-}]_{th}^2 - 7.389[SO_4^{2-}]_{th} + 130.454 \quad \text{for anhydrite} \tag{1}$$

and

$$T\,(^\circ\mathrm{C}) = -31.105[SiO_2aq]_{th}^2 + 111.107[SiO_2aq]_{th} + 5.10939 \quad \text{for chalcedony} \tag{2}$$

2.2. Step II: deviation from ideality

Eqs. (1) and (2) correspond to ideal situations. Natural data are likely to differ from the theoretical curves, which do not account for the effects of pressure, salinity, small crystal size and defect density, which affect mineral solubility. The second step is to quantify this deviation by integrating a global empirical corrective factor, which is mineral-specific and is applied to the solubility data. The value of the corrective factor is adjusted by comparing the calculated temperature-concentration curves in the ideal case with the field data, using end-members representative of the studied geothermal field that were neither diluted nor cooled during their ascent. Numerically, this consists of substituting $[SiO_2aq]_{th}$ and $[SO_4^{2-}]_{th}$ concentrations in the polynomial forms by $\alpha[SiO_2aq]_{th}$ and $\beta[SO_4^{2-}]_{th}$, α and β being the corrective factors. Assuming that $[SO_4^{2-}]_{meas} = \beta[SO_4^{2-}]_{th}$ and $[SiO_2aq]_{meas} = \alpha[SiO_2aq]_{th}$, where 'meas' qualifies the measured data, the newly generated thermometric functions using field concentrations are:

$$T\,(^\circ\mathrm{C}) = 0.1176\left(\frac{1}{\beta}[SO_4^{2-}]_{meas}\right)^2 - 7.3489\left(\frac{1}{\beta}[SO_4^{2-}]_{meas}\right) + 130.45 \tag{3}$$

and

$$T\,(^\circ\mathrm{C}) = -31.105\left(\frac{1}{\alpha}[SiO_2aq]_{meas}\right)^2 + 111.07\left(\frac{1}{\alpha}[SiO_2aq]_{meas}\right) + 5.0939 \tag{4}$$

Note that the quality of the thermodynamic database used, a frequent point of debate, is minimized here because it is integrated in our empirical correction. When the deep end-members have not been sampled, they can nevertheless be approximated, together with the dilution factor, by using correction factors established for hydrothermal systems that present comparable carbonate-evaporite conditions.

2.3. Step III: mixing factor

In this step, we assume that the fluid is a mixture of a deep thermal water and a shallow water. The dilution factor d is introduced in Eqs. (3) and (4) as an unknown parameter:

$$T\,(^{\circ}\mathrm{C}) = 0.1176\left(\frac{d}{\beta}[\mathrm{SO_4^{2-}}]_{\mathrm{meas}}\right)^2 - 7.3489\left(\frac{d}{\beta}[\mathrm{SO_4^{2-}}]_{\mathrm{meas}}\right) + 130.45 \tag{5}$$

and

$$T\,(^{\circ}\mathrm{C}) = -31.105\left(\frac{d}{\alpha}[\mathrm{SiO_2aq}]_{\mathrm{meas}}\right)^2 + 111.07\left(\frac{d}{\alpha}[\mathrm{SiO_2aq}]_{\mathrm{meas}}\right) + 5.0939 \tag{6}$$

Every diluted water is characterised by a value of d. Since the reservoir temperature and the dilution factor are common values for the silica and sulfate thermometric functions, d can be easily calculated by solving the array of equations in the case of dilution by pure water. However, as many shallow waters, even when weakly mineralized, contain appreciable dissolved sulfate and silica, we have to introduce concentrations of the shallow groundwater end-member into Eqs. (5) and (6). By mass balance, the measured concentrations in the fluid can be expressed as a function of the thermal and shallow groundwater end-members:

$$[\mathrm{SO_4^{2-}}]_{\mathrm{meas}} = \frac{1}{d}[\mathrm{SO_4^{2-}}]_{\mathrm{thermal}} + \left(1 - \frac{1}{d}\right)[\mathrm{SO_4^{2-}}]_{\mathrm{shallow}} \tag{7}$$

and

$$[\mathrm{SiO_2}]_{\mathrm{meas}} = \frac{1}{d}[\mathrm{SiO_2}]_{\mathrm{thermal}} + \left(1 - \frac{1}{d}\right)[\mathrm{SiO_2}]_{\mathrm{shallow}} \tag{8}$$

where $1/d$ represents the proportion of the thermal end-member, and $[]_{\mathrm{thermal}}$ and $[]_{\mathrm{shallow}}$ the concentrations in thermal and shallow groundwater end-members, respectively; $[\mathrm{SO_4^{2-}}]_{\mathrm{meas}}$ and $[\mathrm{SiO_2}]_{\mathrm{meas}}$ in Eqs. (7) and (8) are then introduced into Eqs. (5) and (6) to obtain:

$$T\,(^{\circ}\mathrm{C}) = 0.1176\left\{\frac{d}{\beta}\left(\frac{1}{d}[\mathrm{SO_4^{2-}}]_{\mathrm{thermal}} - \left(1 - \frac{1}{d}\right)[\mathrm{SO_4^{2-}}]_{\mathrm{shallow}}\right)\right\}^2 - 7.3489\left\{\frac{d}{\beta}\left(\frac{1}{d}[\mathrm{SO_4^{2-}}]_{\mathrm{thermal}} - \left(1 - \frac{1}{d}\right)[\mathrm{SO_4^{2-}}]_{\mathrm{shallow}}\right)\right\} + 130.45 \tag{9}$$

and

$$T\,(^{\circ}\mathrm{C}) = -31.105\left\{\frac{d}{\alpha}\left(\frac{1}{d}[\mathrm{SiO_2aq}]_{\mathrm{thermal}} - \left(1 - \frac{1}{d}\right)[\mathrm{SiO_2aq}]_{\mathrm{shallow}}\right)\right\}^2 + 111.07\left\{\frac{d}{\alpha}\left(\frac{1}{d}[\mathrm{SiO_2aq}]_{\mathrm{thermal}} - \left(1 - \frac{1}{d}\right)[\mathrm{SiO_2aq}]_{\mathrm{shallow}}\right)\right\} + 5.0939 \tag{10}$$

The solution of the two equations yields the temperature and the contribution of each end-member to the mixture.

2.4. Step IV: conductive cooling

The method also makes it possible to estimate the extent of conductive cooling, if any. Once the mixing proportion between the thermal member ($1/d$) and the cold shallow water ($1 - 1/d$) is calculated, the temperature of the mixture can be computed considering an adiabatic process. Assuming that no exo- and/or endothermic reactions occur upon mixing of the waters (which is likely the case for relatively low-salinity thermal and shallow waters), the temperature of the mixed fluid is close to the value obtained by balancing mass and temperature of the contributing end-members (see Levet et al., 2002). The spring temperatures controlled by an adiabatic mixing process may be expressed by a simple binary equation:

$$T_{\text{adiabatic}} = \frac{1}{d} T_{\text{thermal}} + \left(1 - \frac{1}{d}\right) T_{\text{shallow}} \tag{11}$$

where $T_{\text{adiabatic}}$ represents the water temperature at the spring outlet in the case of an adiabatic mixing process, T_{thermal} the temperature of the aquifer calculated with one of the solubility equations corrected using the empirical correction and dilution factors, and T_{shallow} corresponds to the temperature of the shallow groundwater end-member. The comparison of the calculated temperature ($T_{\text{adiabatic}}$) with the spring temperature (T_{spring}) is an indicator of conductive cooling.

The details and potential applications of the method are illustrated in the following examples.

3. Application to the Bagnères-de-Bigorre hydrothermal system, France

3.1. Description of the spa and chemical data

The Bagnères-de-Bigorre spa is located within a small sedimentary basin in the central part of the French North Pyrenean Zone (Levet et al., 2002). The area presents major faults, numerous thermal springs and gas emanations. The thermo-mineral springs are hosted in Mesozoic limestones, dolomites, marls, clays and evaporites.

The spa area has two types of waters (from Groups I and II) corresponding to two different hydrothermal systems (Levet et al., 2002), which are separated by an impermeable lower Cretaceous clayey flysch hydrologic barrier. Waters from Groups I and II are both of SO_4-Ca-Cl type, but present contrasting salinities (TDS values) and temperatures (Table 1). According to Levet et al. (2002), the chemical composition of both groups derives mainly from dissolution of Triassic evaporites (anhydrites and halites). The saturation indices indicated that the warmer waters (50 °C) are close to equilibrium with anhydrite, while the colder ones (20 °C) are undersaturated with respect to anhydrite, suggesting that they did not equilibrate during ascent. On the other hand, the waters are all undersaturated with respect to halite although they display an Na/Cl ratio equal or close to unity. Among the 12 springs, some of the thermal waters from Group I and all of the Group II waters are diluted by weakly mineralised cold groundwaters (7–11 °C), named Group III, which is of the HCO_3-Ca type. The mixing proportions between Groups I and III waters were calculated by Levet et al. (2002) using binary mixing equations, the Cl and Sr content and the $^{87}Sr/^{86}Sr$ isotopic composition of the undiluted Group I waters (Table 1).

The deep thermal end-member was well represented by the fluids tapped from 150-m deep drillholes. Local shallow dilution with Group III waters is responsible for variations in salin-

Table 1
Data from the literature and results of calculations for three low-temperature geothermal systems. nd, not determined

Reference	T_{spring} (°C)	pH	HCO_3^- (mmol/kg)	Cl^- (mmol/kg)	SO_4^{2-} (mmol/kg)	K^+ (mmol/kg)	Ca^{2+} (mmol/kg)	Na^+ (mmol/kg)	Mg^{2+} (mmol/kg)	SiO_2 (mmol/kg)	TDS (mg/l)	Dilution factor calculated with binary mixing equations based on		Treservoir from Eqs. (5) or (6) (°C)	Dilution factor (d) from Eq. (7) or (8)	Tadiabatic from Eq. (11) (°C)	Dilution factor (d) from Eq. (12)
												[Cl]	[Sr] and $^{87}Sr/^{86}Sr$				
Bagnères-de-Bigorre spa, France (Levet et al., 2002)																	
Group I (1996)																	
1- Lasserre	20.9	7.5	3.01	1.09	8.19	0.08	8.72	1.22	1.41	0.46	1423	2.96	1.92	56.4	1.74	36.6	1.75
2- Saint-Roch	31.4	8.2	2.00	3.05	15.80	0.12	12.81	2.98	2.95	0.81	2404	1.03	1.08	54.0	0.94	56.7	0.94
3- Grands Bains	29.0	7.4	2.62	2.19	11.56	0.08	9.60	2.12	2.18	0.61	1836	1.44	1.32	54.8	1.27	45.3	1.27
4- Soubies	47.7	7.3	2.17	3.18	16.25	0.10	13.21	3.01	3.00	0.71	2479	1.01	1.03	50.3	0.98	51.1	0.98
5- Reine	44.7	6.6	2.16	3.10	15.87	0.10	13.17	2.99	3.01	0.74	2437	1.01	1.00	51.7	0.98	52.7	0.98
6- La Tour	43.1	7.2	2.43	2.59	14.65	0.11	12.50	2.65	2.80	0.68	2278	1.21	1.09	51.9	1.06	49.7	1.06
7- Régina	49.9	7.11	1.91	3.11	16.08	0.09	13.16	3.03	2.91	0.68	2440	1.01	1.08	49.6	1.00	49.6	1.00
8- Cazaux 1	45.7	7.0	2.07	3.16	16.03	0.07	13.16	3.13	2.91	0.64	2448	1.01	1.03	48.4	1.03	47.4	1.03
9- Cazaux 2	49.7	6.9	2.01	3.15	15.83	0.10	13.30	3.08	2.96	0.67	2432	1.01	1.00	49.6	1.02	49.0	1.02
10- Cazaux 3	33.9	7.3	nd	3.11	15.78	0.05	13.34	3.08	2.99	0.72	nd	1.01	nd	51.2	0.99	51.5	0.99
Group I (1998)																	
11- Soubies	46.2	6.9	2.66	3.19	16.89	0.14	14.34	3.29	3.40	0.60	2633	0.98	nd	45.7	1.02	45.0	1.02
12- Reine	46.9	6.8	2.61	3.12	16.52	0.12	14.14	3.30	3.30	0.65	2581	1.01	nd	48.0	1.00	47.9	1.00
13- Régina	49.0	6.9	2.49	3.15	16.86	0.13	14.23	3.31	3.31	0.69	2612	1.00	nd	48.9	0.97	50.2	0.97
14- Cazaux 1	45.5	7.1	2.59	3.12	16.25	0.14	13.90	3.30	3.25	0.52	2544	1.01	nd	43.5	1.10	40.3	1.10
Group I (2000)																	
15- Lasserre	20.5	7.5	3.06	1.33	7.37	0.09	7.33	1.60	1.56	0.50	1242	2.41	nd	60.8	1.79	38.4	1.80
16- Reine	49.0	6.9	1.91	3.04	15.23	0.12	13.12	3.44	2.92	0.86	2436	1.03	nd	56.4	0.94	59.5	0.94
17- Régina	49.9	7.1	1.76	2.99	15.58	0.12	13.28	3.40	2.98	0.85	2395	1.05	nd	55.6	0.93	59.0	0.93
Group II (1996)																	
18- Montagne	32.6	7.5	2.41	3.37	4.80	0.07	4.98	2.98	0.97	0.36	1021	nd	nd	63.6	2.60	30.6	2.63
19- Lavoir	20.5	7.9	2.49	1.87	2.51	0.03	3.33	1.55	0.52	0.22	642	nd	nd	67.1	4.64	22.3	4.76
Group II (1998)																	
20- Montagne	33.0	7.1	2.70	5.49	6.54	0.12	6.96	5.03	1.43	0.44	1421	nd	nd	63.1	1.93	37.5	1.94
21- Lavoir	21.4	6.5	3.01	2.59	3.21	0.06	4.06	2.89	0.73	0.25	832	nd	nd	67.1	3.63	25.7	3.70
Group II (2000)																	
22- Montagne	33.0	7.1	1.56	4.60	5.93	0.08	6.37	4.50	1.24	0.52	1220	nd	nd	67.1	1.97	39.0	1.98
23- Lavoir	20.5	7.2	1.82	1.84	2.46	0.04	3.61	1.92	0.58	0.27	617	nd	nd	72.5	4.25	24.7	4.35
Group III: Shallow groundwater end-member																	
24- Verte	9.5	6.5	0.87	0.07	0.05	0.01	0.24	0.15	0.21	0.01	79						

Acquarossa thermal system, Switzerland (Pastorelli et al., 1999)																
SC—Sato Central	23.9	6.6	10.84	0.15	16.15	0.46	16.58	0.83	3.21	0.68	3000	nd	nd	60.4	1.00	60.6	1.00
AL—Albergo	25.0	6.4	9.38	0.17	14.06	0.31	14.45	0.77	2.76	0.64	2620	nd	nd	61.4	1.11	55.4	1.12
BR—Brenno	19.0	6.7	9.61	0.08	11.46	0.35	12.18	0.78	2.93	0.50	2290	nd	nd	58.5	1.39	42.4	1.45
S1—Soia 1	15.3	6.0	18.03	0.29	11.56	0.95	13.45	1.25	4.46	0.65	2950	nd	nd	65.9	1.22	54.0	1.25
S2—Soia 2	10.7	6.9	18.36	0.33	10.36	0.86	13.03	1.03	4.50	0.49	2830	nd	nd	59.7	1.48	40.5	1.52
Shallow groundwater end-member																	
7	7.0	8.3	1.26	0.01	0.07	0.03	0.69	0.04	0.43	0.16	169						
Middle Jurassic aquifer, Paris Basin, France (Matray et al., 1994)																	
G1	56.0	6.6	9.29	180.56	6.57	1.72	7.95	176.52	5.58	0.44	12400	nd	nd	80.9	1.84	48.6	1.84
G3	71.6	6.3	5.21	400.28	9.67	3.20	25.88	342.61	14.67	0.57	25100	nd	nd	77.9	1.34	60.7	1.34
G36	78.0	6.6	4.75	570.14	12.92	3.79	43.00	471.30	14.83	0.77	35000	nd	nd	78.1	1.00	78.3	1.00
Rapolano thermal system, Italy (Minissale et al., 2002)																	
Terme s. Giovanni	39.9	6.7	47.00	6.37	13.33	1.32	18.00	18.04	9.33	0.46	5901	nd	nd	80.2	0.99	80.6	1.00
Cemetery well	30.1	6.4	46.39	7.55	13.75	1.18	20.15	17.83	9.08	0.53	6011	nd	nd	83.4	0.92	92.0	0.89
Terme Querciolaie	35	6.4	26.61	2.65	5.90	0.44	11.60	5.70	6.88	0.43	3111	nd	nd	93.6	1.66	63.2	1.58
Bagni Freddi 1	25.4	6.3	32.61	5.58	8.13	0.76	16.28	10.30	6.00	0.36	4093	nd	nd	82.9	1.48	57.8	1.54
Bagni Freddi 2	10.4	6.5	24.39	6.48	16.21	0.91	19.70	11.83	6.58	0.61	4616	nd	nd	84.0	0.79	108.5	0.75
Podere Cassarota (spring)	15	7.0	10.51	2.37	2.27	0.26	4.73	3.17	1.63	0.35	1298	nd	nd	102.0	3.02	40.4	3.10
Podere Cassarota (well)	17	6.9	10.70	2.48	2.42	0.26	5.38	3.22	1.58	0.16	1372	nd	nd	62.0	4.28	17.4	8.02
Podere Casalino	13.5	7.0	10.70	1.32	2.34	0.10	6.70	1.61	1.50	0.37	1370	nd	nd	102.7	2.88	42.3	2.93
Podere San Giuseppe	13.5	7.1	11.39	3.27	4.00	0.21	5.50	5.04	2.67	0.28	1652	nd	nd	88.0	2.49	39.1	2.74
Toricella	18	7.2	9.00	2.54	2.19	0.29	4.88	2.96	2.04	0.19	1273	nd	nd	80.6	4.15	22.6	6.01
Capannacce	14	7.0	9.51	2.31	2.10	0.07	5.10	2.65	1.13	0.28	1209	nd	nd	97.8	3.53	33.3	3.89
Capannacce pozzo	17	7.2	7.90	1.75	1.73	0.09	4.10	2.26	1.00	0.18	1008	nd	nd	81.8	4.80	20.6	7.39
Fontpietra	16	7.3	8.20	3.10	1.27	0.47	5.08	2.83	0.63	0.23	1177	nd	nd	98.9	4.94	25.1	6.21
Fontpietra 2	17	7.1	8.30	3.21	1.38	0.42	5.20	3.13	0.63	0.23	1188	nd	nd	97.9	4.76	25.7	5.93
Shallow groundwater end-member																	
Le Fontacce	11.0	7.2	3.70	0.31	0.15	0.10	1.50	0.39	0.46	0.13	359						

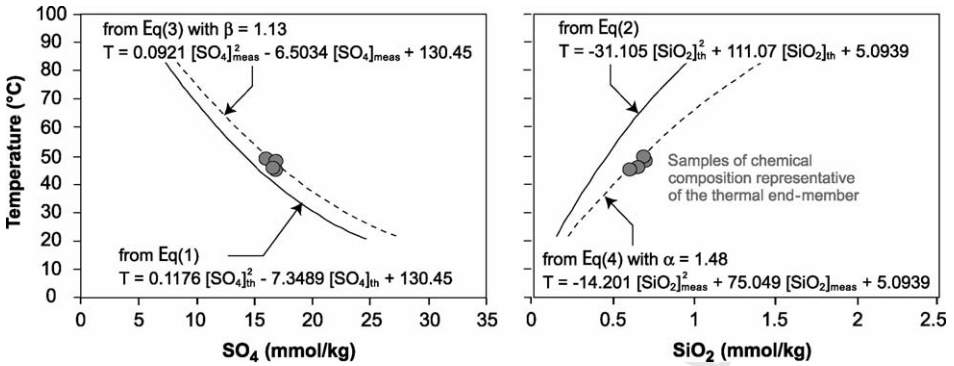

Fig. 2. Temperature vs. concentration relationships showing chalcedony and anhydrite solubility curves computed from Eqs. (1)–(4) for the Bagnères-de-Bigorre hydrothermal system.

ity (617–2633 mg/l), and probably in wellhead temperature (20.9–49.9 °C) in Group I waters. The reservoir temperature was preliminarily estimated around 55–64 °C from Group I waters by applying the Pastorelli et al. (1999) method on the non-diluted fluids. For Group II waters, no mixing or aquifer temperature calculations were performed, as the deep thermal end-member of this hydrothermal system could not be distinguished.

3.2. Results and interpretation

Because the waters of Groups I and II are from similar geologic settings, we assume that the effects of pressure, salinity, small crystal size and defect density influence the solubility of anhydrite and chalcedony by the same amount. We can thus apply the same corrective factors α and β to both groups. A priori, waters taken from drillholes and showing evidence of non-dilution and non-conductive cooling, and spring waters having high outlet temperatures, Cl and SO_4 contents and TDS, will be considered the best candidates for thermal end-member. We therefore used the data of Soubies (samples 4 and 11), Reine (sample 12) and Régina (samples 7 and 13). The calculated α and β assume the values of 1.48 and 1.13, respectively. The corresponding solubility-temperature relations are determined using Eqs. (3) and (4) and are shown in Fig. 2. For each of the waters (diluted or not), the values of d and the aquifer temperature were calculated using Eqs. (5) and (6) and are reported in Table 1.

At this stage we did not take into account the composition of the shallow groundwaters, given their very low sulfate and silica content. It is apparent that the calculated aquifer temperatures of the diluted waters of Group I are close to those of undiluted waters. The d values of Group I waters were also compared with the dilution factors calculated using the binary mixing equations based on strontium and chlorine data reported by Levet et al. (2002). Table 1 shows a good correspondence (maximum difference: 13%) between the dilution factors calculated by solving Eqs. (5) and (6) and by using the strontium data. The correspondence is lower with factors based on Cl data, particularly as regards the most diluted waters (Lasserre, Grands Bains, and La Tour). For Group II, the mean estimated aquifer temperature is 67 °C, and the salinity between 617 and 1421 mg/l, which are different from those of Group I (52 °C and 1242–2633 mg/l, respectively). This also suggests that Group II waters originated from a deeper, hotter reservoir (Levet et al., 2002).

Table 1 also shows the theoretical temperature of adiabatically mixed waters ($T_{\text{adiabatic}}$ in Eq. (11). In accordance with data given by Levet et al. (2002), we assumed an average temperature

of 10 °C for the shallow waters ($T_{shallow}$). For most of the undiluted samples (4, 7, 11, 12, 13) there is a good correlation (within 5 °C), between measured (T_{spring}) and calculated temperatures ($T_{adiabatic}$); see Table 1. This suggests that conductive cooling is negligible for these springs (except for the Saint-Roch spring sampled in a pool), probably because of a rapid ascent of the waters through the numerous local faults acting as preferential flow paths.

3.3. Influence of the composition of the shallow water

When solving Eqs. (5) and (6) in the preceding calculations, we assumed that the shallow groundwater is free of dissolved silica and sulfate. In order to test the influence of shallow water composition, we performed calculations by including the sulfate and silica concentrations of the Group III waters (Table 1: Verte; sample 24) in Eqs. (9) and (10). The dilution factor is calculated by setting Eq. (9) equal to Eq. (10), and obtaining d from Eq. (12):

$$\begin{aligned} & d^2\{0.0921([SO_4^{2-}]_{thermal} - [SO_4^{2-}]_{shallow})^2 + 14.201([SiO_2]_{thermal} - [SiO_2]_{shallow})^2\} \\ & - d\{(0.1842[SO_4^{2-}]_{shallow} - 6.65034)([SO_4^{2-}]_{thermal} \\ & - [SO_4^{2-}]_{shallow}) - ([SiO_2]_{thermal} - [SiO_2]_{shallow})(75.049 - 28.402[SiO_2]_{shallow})\} \\ & + \{0.0921([SO_4^{2-}]_{shallow})^2 - 6.6504[SO_4^{2-}]_{thermal} + 125.3561 + 14.201([SiO_2]_{shallow})^2 \\ & - 75.049[SiO_2]_{shallow}\} = 0 \end{aligned} \quad (12)$$

It is obvious that these corrections make sense only when the dilution rate is significant. In the case of mixed water, we have tested several values for aqueous sulfate and silica concentrations, up to twice the value of the Group III shallow groundwater end-member. The results were not fundamentally different from those reported in Table 1.

The Bagnères-de-Bigorre example illustrates the potential of the proposed coupled anhydrite-chalcedony geochemistry method.

4. Application to the Acquarossa thermal system, Switzerland

The Acquarossa hydrothermal area is located in the Ticino canton of southern Switzerland and is described by Pastorelli et al. (1999). There are three thermal (SC, AL, BR) and two cold (S1 and S2) mineral springs of Ca-SO_4 to Ca-SO_4-HCO_3 chemical composition, and several low-salinity (67–469 mg/l) cold springs of HCO_3-Ca type.

The mineral spring waters (S1 and S2) display cold to moderate discharge temperatures (between 10.7 and 25 °C; TDS from 2290 to 3000 mg/l; and near-neutral pH values of 6.0–6.9 (Table 1). The chemical composition of the thermal springs (SC, AL, BR) originates from dissolution of carbonate and anhydrite-bearing Triassic evaporite rocks at depth, whereas the cold spring waters acquire their chemistry through interaction with shallow gneissic-carbonate rocks. Despite their distinct discharge areas, the Acquarossa (SC, AL and BR) and Soia (S1 and S2) springs likely originate from the same aquifer, and probably rise quickly to the surface along fractures, without any major alteration of their physical and chemical characteristics. Thus, the variations of chemical composition of these spring waters are mainly due either to dilution with the cold HCO_3-Ca or Ca-SO_4 springs, or to different partial pressures of CO_2 (recognised as a separate gas phase in the S1, S2, SC and BR springs) governing the HCO_3/SO_4 ratio given

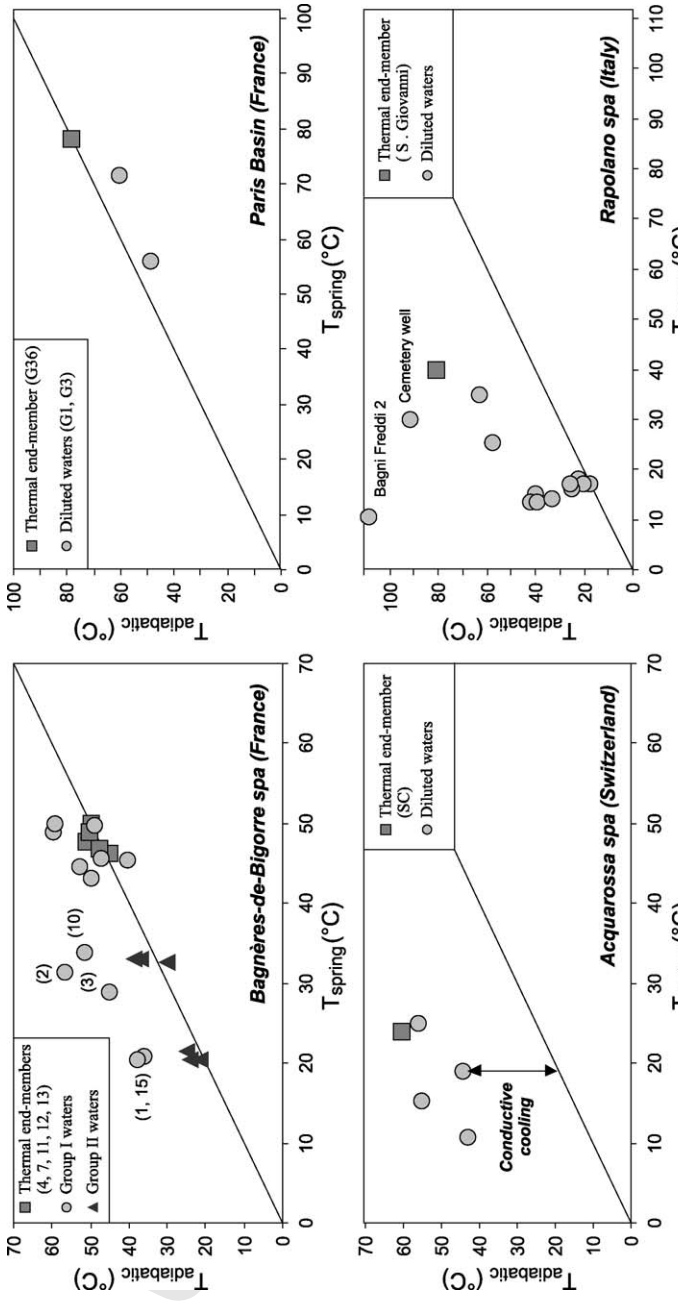

Fig. 3. Discharge spring water temperatures vs. temperatures assuming adiabatic mixture (i.e., theoretically calculated spring temperature) for the studied geothermal systems. For more details see Table 1.

by the reaction:

$$CaCO_3 + CO_2 + SO_4^{2-} + H_2O = CaSO_4 + 2HCO_3^{2-} \quad (13)$$

Pastorelli et al. (1999) recognized spring SC as the most representative of the deep thermal end-member, and used it to find the deep aquifer temperature. They found that equilibrium with respect to anhydrite, calcite and chalcedony was reached close to 60 °C in the deep aquifer, which corresponds to the temperature at 1.5 km depth, assuming a normal thermal gradient of 30 °C/km and an average surface temperature of 15 °C.

As in the case of the Bagnères-de-Bigorre hydrothermal system, we applied the combined solubility of anhydrite and chalcedony to calculate the dilution proportions and the extent of conductive cooling. We used the chemical composition and outlet temperatures of spring SC and the shallow groundwater end-member given in Table 1 (i.e., 7), as the undiluted deep and shallow groundwater end-members, respectively. Parameters α and β were computed to be 1.14 and 1.37, respectively.

The five thermal springs display a homogeneous aquifer temperature close to 60 °C (Table 1), in agreement with the results of Pastorelli et al. (1999). The calculated proportions of shallow water in springs AL, BR, S1 and S2 are significant (as suggested, but not quantified, by Pastorelli et al., 1999), with values of almost 11, 31, 20 and 36%, respectively. In Fig. 3 the adiabatic mixing temperatures based on Eq. (11) are compared to the measured outlet temperatures. Our model indicates that all of the thermal spring waters at Acquarossa were affected by 24–39 °C conductive cooling during their ascent.

5. Application to the Middle Jurassic Aquifer of the Paris Basin, France

The intracratonic sedimentary Paris Basin has a radius of approximately 350 km and a maximum sediment thickness of 3000 m. The basin's Dogger Aquifer (Middle Jurassic) is a 200–300 m thick predominantly carbonate reservoir, confined between two low-permeability marl formations. The chemical composition of the Dogger waters (Table 1) is controlled by a complex mixing process. At the bottom of the aquifer, the salt load results from the migration of secondary Triassic brines via vertical fractures. The Triassic layers are mainly composed of evaporites (halite and anhydrite), sandstones, dolomites and claystones. We therefore expect the Dogger Aquifer waters to be in equilibrium with anhydrite. At shallower depth, these waters are diluted by infiltrated meteoric waters. The maximum aquifer temperature (85 °C) was measured at Meaux, north-east of Paris (Rojas et al., 1987). This area, in the centre of the Paris basin, also corresponds to the zone in which the waters have the highest TDS values and has been interpreted as reflecting little dilution by the infiltrated meteoric waters (Matray, 1988).

Matray et al. (1994) reported the chemical composition of a representative set of geothermal waters (G1, G3 and G4; Table 1) from the Dogger Aquifer, essentially of Na-Ca-Cl type. They have discharge temperatures of 56, 71.6 and 78 °C, respectively, which correlate with their TDS values, ranging between 12.4 and 35 g/l (Table 1).

Our model was adjusted by using the composition of water G36, which shows the highest discharge temperature, saline load, sulfate and silica contents. Since Matray et al. (1994) did not report the composition of the shallow groundwaters, we set by default the sulfate and silica concentrations to zero for the shallow groundwater end-member, and the temperature to 10 °C. Parameters α and β were calculated to be 0.88 and 1.58, respectively. The low value for α reflects the high temperature of this system, which probably favours crystalline siliceous phases. By

contrast, the high value for β demonstrates the high salinity of the waters. We found a very similar reservoir temperature of $79 \pm 2\,^{\circ}C$ (Table 1) for the three waters (G1, G3 and G36). Our calculations also show that samples G3 and G1 are diluted 26 and 46%, respectively, by shallow waters (assumed to be depleted in SO_4^{2-} and SiO_2), and do not show indications of any significant conductive cooling (Fig. 3).

6. Application to the Rapolano thermal system, central Italy

Central Italy is characterised by a quasi-continuous regional aquifer hosted in Mesozoic carbonate-evaporite sequences (Minissale, 1991). This large groundwater reservoir feeds numerous thermo-mineral springs, which discharge in the various tectonic windows of the central western peri-Tyrrhenian, pre-Apennine belts. Associated with these large regional water discharge areas is the anomalous heat flow generated by magma bodies and the presence of geologic faults that allow the ascent and surface discharge of deep fluids. The chemical composition of the thermal waters (Duchi et al., 1992; Minissale et al., 2002) belonging to this major aquifer can be summarised by (i) a Ca-SO_4 end-member resulting from the interaction of the waters with the anhydrite-bearing Triassic layers, (ii) a Ca-HCO_3-SO_4 end-member also originated from the dissolution of Triassic evaporite minerals, but where strong deep CO_2 fluxes are equilibrated with the aquifer waters, and (iii) a Na-Cl-HCO_3, highly saline end-member, created by leaching or mixing with post-orogenic connate waters from marine formations or with deep secondary brines.

The Rapolano thermal system is located along the eastern border of the Siena-Radicofani Basin, which is a typical Mesozoic sedimentary graben in Tuscany region (Duchi et al., 1992). The area has numerous thermal and cold mineral springs, sometimes associated with a gas phase; their temperatures vary between 9.5 and 39.9 °C. These waters belong to the three characteristic types described above; they often display mixed features, and in most of the thermal springs there is bubbling CO_2. Some springs form large travertine deposits, such as at Rapolano, where travertine is still being mined for the building industry.

All the Rapolano spring waters are of meteoric origin, and are heated at depth because of the anomalous high regional heat flow. As most springs discharge from the fault system at the eastern edge of the Siena-Radicofani graben, which provides fast flow paths, the waters likely maintain the chemical features of the deep aquifer. Moreover, mixing between the waters of the Na-Cl aquifer and the deep carbonate-evaporite reservoir is very limited at Rapolano (Minissale et al., 2002), and the major mixing process affecting the thermal waters along the upflow paths is dilution with weakly mineralised Ca-HCO_3 shallow groundwaters. Minissale et al. (2002) studied this dilution using dissolved boron, Ne and N_2 gas data, but this process was not quantified.

According to Minissale et al. (2002), the San Giovanni thermal spring should be the most representative water of the deep Ca-HCO_3-SO_4 Mesozoic aquifer, as it is the least contaminated by Ca-HCO_3 shallow groundwaters. We used this spring as a reference to adjust Eqs. (3) and (4), by assuming no dilution and an 80 °C equilibrium temperature, as concluded by Chiodini et al. (1995). The deficit of sulfate with respect to HCO_3^- is likely related to carbonate dissolution, enhanced by the exceptionally high CO_2 partial pressure reported for this system (Minissale et al., 2002). On the other hand, the precipitation of travertine at the surface, which is also an exceptional phenomenon at Rapolano, is not thought to affect sulfate concentration, which remains a reliable indicator of the water-anhydrite equilibrium in the deep aquifer. We considered the composition and temperature of "Le Fontacce" spring (Table 1) as representative of the shallow groundwater end-member.

The method was applied to 14 water samples representative as much as possible of the various chemical features of the Rapolano thermal field. The samples were gathered from an area within 3 km north, west and south of the town of Rapolano (Minissale et al., 2002). The calculated aquifer temperatures range from 62 to 102 °C (Table 1).

The scattering of the aquifer temperature values correlates with the large variation in spring temperatures ($R^2 = 0.70$). In contrast to Group II of the Bagnères-de-Bigorre spa, where the calculated temperatures clustered around 67 °C, the results of our model suggest that a more complex thermal system exists at Rapolano, with several upflow paths related to the well-developed fault system at the edge of the graben. The results also indicate that the dilution rates for the Rapolano thermal waters range between 12 and 88%. When comparing the spring water discharge temperatures to the theoretical temperatures that assume adiabatic mixture, it becomes apparent that significant conductive cooling takes place (up to 98 °C; Fig. 3).

7. Concluding remarks

Numerous low-temperature geothermal systems throughout the world are hosted in carbonate-evaporite rocks. Because of their special lithology and the effects of mixing, conventional geothermometers based on chemical equilibrium with the silicates phases cannot be applied to these systems. Even the chalcedony geothermometer cannot be readily used because of dilution with shallow groundwaters.

We propose an empirical, fast and easy method to calculate mixing factors and conductive cooling in (40–100 °C) thermal waters, key parameters in geothermometry and the hydrogeology of geothermal systems. The method constrains the hydrogeologic features by providing estimates on the mixing proportions and aquifer temperature. However, it cannot be applied universally, as it is based on the assumption that the aquifer waters are in equilibrium with respect to chalcedony and anhydrite, which are typical minerals of evaporite facies.

The geothermal fields used here to illustrate the application of our method are located in Mesozoic carbonates, which are mainly made up of limestones and dolomites associated with clays. In these settings, the Triassic evaporites are linked to major tectonic structures (i.e., faults) and therefore may constitute preferential pathways for thermal fluid circulation.

The use of the thermodynamic properties of anhydrite and chalcedony in geothermometry had already been proposed by Pastorelli et al. (1999). In the present study, empirical adjustment of the solubility data to the local hydrochemical and mineralogical conditions has permitted a more exhaustive interpretation of the data. Apart from the determination of aquifer temperature, our approach also allows to estimate dilution effects during ascent and provides evidence of any conductive cooling of the thermal fluids.

Where data are not available on the deep end-member, our method can in some cases be used to determine the temperature and composition of the thermal end-member of mixed fluids. The method, however, requires calibration with data from another geothermal system with comparable lithology and geological setting. The method is not influenced by many of the processes that commonly occur during the ascent of a fluid to the surface or spring, such as CO_2-degassing, conductive cooling, precipitation of carbonates and pH variations.

The four examples discussed in the paper illustrate the potential of the method. However, we want to stress that the results presented here are not definitive interpretations of these geothermal systems, which would require a more complete set of data. Moreover, the uncertainty of the method has not been discussed systematically, mainly because the numerical values we obtained are partly based on empirical adjustments.

Acknowledgements

The authors are very grateful to G. Cortecci and M. Reed for their constructive reviews. They also thank M. Lippmann and M. Dickson for editing and improving the manuscript.

References

Antroddicchia, E., Cioni, R., Chiodini, G., Gagliardi, R., Marini, L., 1985. Geochemical temperatures of the thermal waters of Phlegrean fields (Naples, Italy). Geotherm. Res. Council. Transact. 9 (part I), 287–292.

Arnórsson, S., 1975. Application of the silica geothermometer in low temperature hydrothermal areas in Iceland. Am. J. Sci. 275, 763–784.

Arnórsson, S., 1983. Chemical equilibria in Icelandic geothermal systems-implications for chemical geothermometry investigations. Geothermics 12 (2–3), 119–128.

Arnórsson, S., Gunnlaugsson, E., Svavarsson, H., 1983. The chemistry of geothermal waters in Iceland. III. Chemical geothermometry in geothermal investigations. Geochim. Cosmochim. Acta 47, 567–577.

Azaroual, M., Fouillac, C., Matray, J.M., 1997. Solubility of silica polymorphs in electrolyte solutions. II. Activity of aqueous silica and solid silica polymorphs in deep solutions from the sedimentary Paris Basin. Chem. Geol. 140, 167–179.

Can, I., 2002. A new improved Na/K geothermometer by artificial neural networks. Geothermics 31, 751–761.

Chiodini, G., Cioni, R., Guidi, M., Marini, L., 1991. Chemical geothermometry and geobarometry in hydrothermal solutions: a theoretical investigation based on a mineral-solution equilibrium model. Geochim. Cosmochim. Acta 55, 2709–2727.

Chiodini, G., Frondini, F., Marini, L., 1995. Theoretical geothermometers and P_{CO_2} indicators for aqueous solutions coming from hydrothermal systems of medium-low temperature hosted in carbonate-evaporite rocks. Application to the thermal springs of the Etruscan Swell, Italy. Appl. Geochem. 10, 337–346.

Cioni, R., Fanelli, G., Guidi, M., Kinyariro, J.K., Marini, L., 1992. Lake Bogoria hot springs (Kenya): geochemical features and geothermal implications. J. Geotherm. Volcanol. Res. 50, 231–246.

Debye, P., Hückel, E., 1923. Zur Theorie der Electrolyte, I and II. Physikalische Zeitschrift 24, 185–305.

Degueldre, C., Pfeiffer, H.R., Alexander, W., Wernli, B., Bruetsch, R., 1996. Colloid properties in granitic groundwater systems. I. Sampling and characterization. Appl. Geochem. 11, 677–695.

Duchi, V., Minissale, A., Paolieri, M., Prati, F., Valori, A., 1992. Chemical relationship between discharging fluids in the Siena-Radicofani graben and the deep fluids produced by the geothermal fields of Mt Amiata, Torre Alfina and Latera (central Italy). Geothermics 21 (3), 401–413.

Ellis, A.J., 1979. Chemical geothermometry in geothermal systems. Chem. Geol. 25, 219–226.

Fouillac, C., Michard, G., 1981. Sodium/lithium ratio in water applied to geothermometry of geothermal reservoirs. Geothermics 10, 55–70.

Fournier, R.O., 1977. Chemical geothermometers and mixing models for geothermal systems. Geothermics 5, 41–50.

Fournier, R.O., 1979. A revised equation for the Na/K geothermometer. Geotherm. Res. Counc. Trans. 3, 221–224.

Fournier, R.O., Potter II, R.W., 1979. Magnesium correction to Na-K-Ca chemical geothermometer. Geochim. Cosmochim. Acta 43, 1543–1550.

Fournier, R.O., Potter II, R.W., 1982. A revised and expanded silica (quartz) geothermometer. Geotherm. Res. Counc. Bull. 11, 3–12.

Fournier, R.O., Rowe, J.J., 1966. Estimation of underground temperatures from silica content of waters from hot springs and wet steam wells. Am. J. Sci. 264, 685–697.

Fournier, R.O., Truesdell, A.H., 1973. An empirical Na-K-Ca geothermometer for natural waters. Geochim. Cosmochim. Acta 37, 1255–1275.

Fournier, R.O., Truesdell, A.H., 1974. Geochemical indicators of subsurface temperatures: Part 1. Basic assumptions. J. Res. U.S. Geol. Survey 2, 259–262.

Giggenbach, W.F., 1988. Geothermal solute equilibria. Derivation of Na-K-Mg-Ca geoindicators. Geochim. Cosmochim. Acta 5, 2749–2765.

Hull, C.D., Reed, M.H., Fisher, K., 1987. Chemical geothermometry and numerical unmixing of the diluted geothermal waters of the San Bernardino Valley region of southern California. Geotherm. Res. Counc. Trans. 11, 165–184.

Johnson, J.W., Oelkers, E.M., Helgeson, J.W., 1992. SUPCRT92: a software package for calculating the standard molal thermodynamic properties of minerals, gases, aqueous species and reactions from 1 to 5000 bars and from 0 to 1000 °C. Comp. Geosci. 18, 899–947.

Kharaka, Y.K., Mariner, R.H., 1989. Chemical geothermometers and their application to formation waters from sedimentary basins. In: Naeser, N.D., McCulloh, T.H. (Eds.), Thermal History of Sedimentary Basins. Springer Verlag, New York, pp. 99–117.

Levet, S., Toutain, J.P., Munoz, M., Berger, G., Negrel, P., Jendrzejewski, N., Agrinier, P., Sortino, F., 2002. Geochemistry of the Bagnères-de-Bigorre thermal waters from the North Pyrenean Zone sedimentary environment (France). Geofluids 2, 1–16.

Marini, L., Chiodini, G., Cioni, R., 1986. New geothermometers for carbonate-evaporite geothermal reservoirs. Geothermics 15, 77–86.

Matray, J.M., 1988. Hydrochimie et géochimie isotopique des eaux du réservoir pétrolier du Trias et du Dogger dans le basin de Paris. Thèse de l'Université de Paris-Sud, Orsay, France.

Matray, J.M., Lambert, M., Fontes, J.C., 1994. Stable isotope conservation and origin of saline waters from the Middle Jurassic aquifer of the Paris Basin, France. Appl. Geochem. 9, 297–309.

Millero, F.J., 1982. The effect of pressure on the solubility of minerals in water and seawater. Geochim. Cosmochim. Acta 46, 11–22.

Minissale, A., 1991. Thermal springs in Italy: their relation to recent tectonics. Appl. Geochem. 6, 201–212.

Minissale, A., Vaselli, O., Tassi, F., Magro, G., Grechi, G.P., 2002. Fluid mixing in carbonate aquifers near Rapolano (central Italy): chemical and isotopic constraints. Appl. Geochem. 17, 1329–1342.

Monnin, C., 1990. The influence of pressure on the activity coefficients of the solutes and on the solubility of minerals in the system Na-Ca-Cl-SO_4-H_2O to 200 °C and 1 kbar, and to high NaCl concentration. Geochim. Cosmochim. Acta 54, 3265–3282.

Paces, T., 1975. A systematic deviation from Na-K-Ca geothermometer below 75 °C and above 10^{-4} atm. P_{CO_2}. Geochim. Cosmochim. Acta 39, 541–544.

Palandri, J.L., Reed, M., 2001. Reconstruction of in situ composition of sedimentary formation waters. Geochim. Cosmochim. Acta 65, 1741–1767.

Pang, Z.H., Reed, M., 1998. Theoretical chemical thermometry on geothermal waters: problems and methods. Geochim. Cosmochim. Acta 62, 1083–1091.

Pastorelli, S., Marini, L., Hunziker, J.C., 1999. Water chemistry and isotope composition of the Acquarossa thermal system, Ticino, Switzerland. Geothermics 28, 75–93.

Pitzer, K.S., 1973. Thermodynamics of electrolytes. I. Theoretical basis and general equations. J. Phys. Chem. 77, 268–277.

Reed, M., Spycher, N., 1984. Calculation of pH and mineral equilibria in hydrothermal waters with application to geothermometry and studies of boiling and dilution. Geochim. Cosmochim. Acta 48, 1479–1492.

Rojas, J., Menjoz, A., Martin, J.C., Criaud, A., Fouillac, C., 1987. Development and exploitation of low enthalpy geothermal systems: example of the Dogger in the Paris Basin, France. In: Proceedings of the 12th Workshop on Geothermal Reservoir Engineering, Stanford, CA, pp. 203–212.

Verma, S.P., 2001. Silica solubility geothermometers for hydrothermal systems. In: Cidu, R. (Ed.), Proceedings of the 10th International Symposium on Water–Rock Interaction. June 10–15, vol. 1. Lisse, Villasimius, Italy, pp. 349–352, A.A. Balkema.

Verma, S.P., Santoyo, E., 1997. New improved equations for Na/K, Na/Li and SiO_2 geothermometers by outlier detection and rejection. J. Volcanol. Geotherm. Res. 79, 9–23.

White, D.E., Brannock, W.W., Murata, K.J., 1956. Silica in hot spring waters. Geochim. Cosmochim. Acta 10, 27–59.

Wolery, T., Daveler, S.A., 1992. EQ3/6, A Software Package for Geochemical Modelling of Aqueous Systems. UCRL-MA-110772 PT IV. Lawrence Livermore National Laboratory, Livermore.